Ocular Surface Pathology in Patients Suffering From Mercury Intoxication Is Consistent With Neurogenic Dry Eye Disease

Pilar Cañadas (pilarcanadas.s@gmail.com)
IOBA (Institute of Applied Ophthalmobiology), University of Valladolid, Valladolid, Spain
Yrbani Lantigua Dorville
IOBA (Institute of Applied Ophthalmobiology), University of Valladolid, Valladolid, Spain
Amalia Enríquez-de-Salamanca
CIBER-BBN (Biomedical Research Networking Center Bioengineering, Biomaterials and Nanomedicine), Carlos III National Institute of Health, Spain
Itziar Fernandez
CIBER-BBN (Biomedical Research Networking Center Bioengineering, Biomaterials and Nanomedicine), Carlos III National Institute of Health, Spain
Salvador Pastor-Idoate
IOBA (Institute of Applied Ophthalmobiology), University of Valladolid, Valladolid, Spain
Eva M. Sobas
IOBA (Institute of Applied Ophthalmobiology), University of Valladolid, Valladolid, Spain
Antonio Dueñas
ICIME (Medical Sciences Institute), Medical School, University of Valladolid, Valladolid, Spain
José Luis Pérez-Castrillón
ICIME (Medical Sciences Institute), Medical School, University of Valladolid, Valladolid, Spain
J. Carlos Pastor
IOBA (Institute of Applied Ophthalmobiology), University of Valladolid, Valladolid, Spain
Margarita Calonge
CIBER-BBN (Biomedical Research Networking Center Bioengineering, Biomaterials and Nanomedicine), Carlos III National Institute of Health, Spain

Research Article

Keywords: Corneal esthesiometry, corneal innervation, in vivo confocal microscopy, mercury intoxication, neurogenic dry eye, tear cytokines

Posted Date: January 19th, 2021

DOI: https://doi.org/10.21203/rs.3.rs-146734/v1

Abstract

Purpose: To report ocular surface pathology of patients with acute/subacute mercury intoxication.

Methods: Male workers intoxicated with inorganic mercury were examined for dry eye (DE)-related symptoms. Examinations included Ocular Surface Disease Index questionnaire; tear osmolarity, tear break-up time (T-BUT) and production; mechanical and thermal corneal sensitivity; corneal nerve and dendritic cell density analysis; and analysis of 23 tear cytokines.

Results: Most patients, 63.6%, had severe DE-related symptoms. Tear osmolarity was elevated in 83.4%, and T-BUT was low in 22.7% of patients. Tear production and tear lysozyme concentration were low in 13.6% and 27.3% of cases, respectively. Corneal sensitivity thresholds for mechanical, heat and cold stimuli were higher than controls. Densities of nerves, nerve branching, and dendritic cells were lower than in controls. Patient tear levels of IL-12p70, IL1-RA, RANTES, and VEGF were increased, whereas EGF, IL-6, and IP-10/CXCL10 were decreased. Based on cytokine levels, two clusters of patients were identified. Cluster 2 patients had significantly increased tear levels of 18 cytokines, decreased tear lysozyme, lower nerve branching density, fewer dendritic cells, and higher urine mercury levels.

Conclusions: Mercury poisoning produced previously undescribed ocular surface pathology, similar to neurogenic inflammatory type of DE and different from the more common DE subtypes.

Introduction

Mercury is a metallic element with a high potential for toxicity. Several public health disasters by mercury intoxication (also known as “mercury poisoning”) have been reported, the most well-known of these occurred in Japan in 1956 and was known as Minamata disease. Afterwards, the Minamata Convention on Mercury made the world aware of the environmental and public health issues that mercury pollution represented and that are still present.[1] The most frequent human exposure to water-soluble forms of mercury, such as mercuric chloride or methylmercury, is caused by ingestion of any form of mercury, e.g., contaminated fish, or by inhalation of mercury vapor as an occupational exposure, including coal burning and mining, especially of mercury and gold.[1]

Exposure to different forms of mercury has been associated with adverse health effects.[2] Intoxication due to inhalation of mercury vapor, a form of inorganic mercury, produces the most harmful effects, as up to 80% of the inhaled mercury is absorbed and rapidly oxidized to other forms. Oxidized mercury vapor becomes lipid soluble, so the potential exists for bioaccumulation in the renal cortex, liver, and especially in the brain, where it has been estimated that the half-life can be as long as 20 years.[3] Even though the principal target organ of mercury vapor is the brain, functional degradation of peripheral nerves, and of the renal, immune, endocrine, and muscle systems, and several types of dermatitis have been described.[4]

Numerous ophthalmic findings due to mercury toxicity and its action on the retina and optic nerve have been reported for both chronic and acute exposures. These include decreased night vision, decreased color vision and contrast sensitivity, central visual impairment, progressive visual field constriction, and optic atrophy.[5] Less frequent symptoms and signs such as photophobia, blepharospasm, nystagmus, and mercury deposits on the anterior capsule of the lens (mercurialentis) and corneal stroma have also been reported in some cases of chronic intoxication.[5] Ocular surface pathology due to acute and chronic exposure to mercury exposure has only been vaguely described in experimental models.[6–8] However, there are no published studies reporting human ocular surface effects.

At the end of 2012, 49 workers in Northern Spain were accidentally exposed to dangerous levels of mercury vapor. Blood and urine levels of mercury were above the recommended biological limits for occupational exposure, and acute and subacute (acute/subacute) mercury vapor intoxication was confirmed. Most of these patients were referred to the University of Valladolid, Spain, between 1 and 2 years later, and those with ophthalmic complaints were referred to the Institute of Applied Ophthalmobiology (IOBA), University of Valladolid, Valladolid, Spain. In this study, we aimed to find the origin of the patients’ chronic ocular surface-related symptoms. Based on the known mechanisms of mercury-based pathogenesis, we hypothesized the presence of neurogenic inflammation of the ocular surface. Therefore in addition to the usual clinical tests, to assess the

presence of a neurogenic component in the mercury-dependent ocular surface pathology, we added tests for corneal mechanical and temperature sensitivity, corneal nerve morphology, and inflammatory molecules in the tears.

Methods

2.1. Patients

This study was approved by the Institutional Review Board and by the Ethics Committee of the Valladolid University Clinical Hospital. All enrolled patients were informed of the aims of the study, and their written consent was obtained. All research was performed in accordance with relevant regulations and in accordance with the Declaration of Helsinki.

Acute/subacute mercury vapor intoxication occurred in 49 male workers accidentally exposed to dangerous mercury vapor levels for 14 consecutive days in a metal manufacturing plant in Northern Spain between November 19 and December 2, 2012. In the days after exposure, many of the workers reported physical complaints, mainly asthenia, headache, epigastric and abdominal pain, cough, bitter taste, dental pain, and gum inflammation and bleeding. Some of the workers also had ocular symptoms such as irritation, redness, burning, foreign body sensation, and light photophobia. Blood and urine mercury levels were measured during the second week of the exposure, and were above the recommended biological limits for occupational exposure, reaching maximum range levels between 252.62 and 507.47 μg/L in blood (normal, < 10 μg/L) and between 93.61 and 245.57 μg/g creatinine in urine (normal, < 30 μg/g creatinine). Some weeks before occupational exposure, random urine samples (n = 17) detected mercury levels below 3 μg/g creatinine in those workers. The diagnosis of acute/subacute intoxication with mercury vapor was confirmed by the post-exposure clinical analyses.

Between September 2013 and December 2014, 44 of the original 49 intoxicated patients were referred to the Clinical Toxicology Unit of the Institute of Medical Sciences at the University of Valladolid for an independent evaluation. Of those, 29 patients had ocular symptomatology and were immediately referred to IOBA and evaluated for enrollment. All referred patients had vision and retinal-related symptoms, which have been studied by our colleagues, and ocular surface-related symptoms.

All of the referred patients received medical care and were evaluated for inclusion in this study. The only inclusion criterion was that patients had to have reported their ocular surface symptoms after the mercury intoxication. The exclusion criteria were (1) pre-existing ocular surface symptoms; (2) use of artificial tears or any other topical medication before mercury intoxication; (3) use of any topical medication other than artificial tears 4 weeks before enrollment or 3 months before enrollment in the case of either topical cyclosporine or tacrolimus; (4) use of contact lenses in the previous 3 months; (5) any other ocular surface disease; or (6) any previous ocular surgery.

2.2. Clinical evaluation and tear sample collection

Both eyes were evaluated between 10 am and 2 pm. The temperature of the examination room was always set at 19–21ºC, and the relative humidity was between 50–60%. Clinical evaluation and subjective tests were always performed by the same examiner in a single visit and in the sequence detailed below.

2.2.1. Ocular surface-related symptom questionnaire

The Ocular Surface Disease Index (OSDI) questionnaire was self-administered, and based on the score, each patient was categorized as having no symptoms (score 0–12) or as having mild (score 13–22), moderate (score 23–32 points), or severe (score 33–100) ocular surface-related symptoms.[9]

After that, we asked each patient which eye he considered the most symptomatic. That eye was used for tear sampling, osmolarity measurement, esthesiometry, microscopy, and in statistical analyses of the clinical tests. If both eyes were equally symptomatic, the eye was selected by computer-generated randomization.

2.2.2. Tear sample collection for molecular analysis

We followed our previous protocol in which unstimulated basal tear samples were collected non-traumatically from the external canthus.[10, 11] One microliter of tear sample was collected with a glass capillary micropipette (Drummond, Broomall, PA, USA). Each sample was then diluted 1:10 in ice-cold Cytokine Assay Buffer (Milliplex, Millipore Merck Life Science SLU, Madrid, Spain). Tear samples were kept cold (4 °C) during collection and then stored at − 80 °C until assayed.

2.2.3. Tear osmolarity

Ten minutes after the tear sample collection, the osmolarity was assessed by the TearLab osmometer (TearLab Corporation, San Diego, CA, USA) in a 50-nL tear sample collected from the external canthus. Values above 308 mOsm/L were considered abnormal. [12]

2.2.4. Conjunctival bulbar hyperemia

Ten minutes after the tear sample collection for osmometry, the nasal and temporal conjunctivas were assessed independently with a slit-lamp biomicroscope based on the Efron scale (0–4 score). The final score was the average of the nasal and temporal values. [12]

2.2.5. Tear break-up time (T-BUT)

Five minutes after slit-lamp biomicroscopy, tear stability was assessed by T-BUT. After instillation of 5 µL of 2% sodium fluorescein, the time between the last of three blinks and the appearance of the first dry spot was measured three times, and the mean value was recorded. Values below 7 seconds are currently considered abnormal.[12]

2.2.6. Ocular surface integrity

Approximately 2 minutes after fluorescein instillation for T-BUT, corneal and conjunctival integrity were evaluated with fluorescein and lissamine green staining, respectively. The Oxford scheme (0–5 score) for grading the staining of both areas was used.[12]

2.2.7. Tear production

Five minutes after the previous test, tear production was assessed with two different tests: tear lysozyme level assay and Schirmer's test without topical anesthesia. The tear lysozyme concentration test was performed as previously detailed, and values of less than 1,000 µg/ml were considered indicative of low tear production.[13] Then, after 5 minutes, the Schirmer test was performed by placing a sterile strip (I-DEW tear strips, Entod Research Cell UK, Ltd, London, UK) in the lateral canthus of the inferior lid margin, and the length of wetting was measured after 5 min. Results below 5-mm length were considered abnormal. [12]

2.3. Corneal sensitivity

Twenty minutes after, corneal sensitivity was measured with a prototype Belmonte's non-contact gas esthesiometer as previously reported by our group.[14, 15] The corneal threshold for mechanical and thermal (cold and heat) sensitivities was determined in the central cornea using the method of levels. Three-second air pulses of adjustable flow rate and temperature were applied to the center of the cornea for determining corneal sensitivity thresholds. Mechanical stimulation was always first and consisted of a series of variable flows of medicinal air (0–200 mL/min). Thermal thresholds were determined by heating or cooling the air to produce changes in basal corneal temperature of ± 0.1ºC, with a 10 mL/min flow below the mechanical threshold. Immediately after each stimulation pulse, the subject was asked to report the presence or absence of sensation. The order of heat and cold threshold measurement was randomized. Results were compared with a separate, but similarly aged (38.5 ± 8.2 years, $p = 0.1622$) control group of 20 healthy males from our files.[14, 15, 16] Each subject in the control group had an OSDI ≤ 12, corneal staining < 1 (Oxford scale), T-BUT ≥ 7 seconds, and a Schirmer test ≥ 5 mm/5 min.

2.4. In vivo confocal microscopy (IVCM)

Ten minutes after measuring sensitivity, and after applying topical anesthesia (0.1% tetracaine and 0.4% oxibuprocaine, Anestésico Doble Colirio; Alcon-Cusí, El Masnou, Barcelona, Spain), laser scanning IVCM of the cornea was performed using the Rostock cornea module of the Heidelberg Retina Tomograph 3 (Heidelberg Engineering GmbH, Heidelberg, Germany). At least

three good quality, non-overlapping images from the sub-basal nerve plexus of the central cornea were obtained using sequence and/or volume scans were used for the analysis. Two masked observers analyzed the following: (1) nerve morphology parameters of density, length, branching density, and grade of tortuosity; (2) density of dendritic cells; (3) presence of neuromas; and (4) reflectivity from the confocal images, as an index of optic densitometry or transparency of cornea.[17] The mean value between the two observers for each parameter was computed for statistical analysis.

Nerve density (n/mm^2) and length (mm/mm^2) were measured using the plugin NeuronJ (http://www.imagescience.org/meijering/software/neuronj/) from the ImageJ software (https://ima gej.nih.gov/ij/), which allows semi-automated tracing of nerve fibers and provides quantification. The number of nerve branch points and dendritic cells (identified in the sub-basal nerve plexus by their distinctive features, i.e., bright cell bodies with dendritic form structures), were manually determined using the multipoint tool of the ImageJ software, and the densities calculated (n/mm^2) as described in a previous study.[18] The grade of nerve tortuosity was evaluated according to the scale (0–4) reported by Oliveira-Soto and Efron[19] for main nerves. The histogram of each image based on the ImageJ plugin was used to obtain the mean reflectivity or optic densitometry.[17] These parameters were compared with well-established values for normal corneas and performed with the same type of confocal microscope. Specifically, we used data from Giannacare et al.[20] for nerve length, and from our group for nerve density, density of nerve branches, density of dendritic cells,[18] and nerve tortuosity and reflectivity.[17]

2.5. Analysis of tear cytokine concentrations

A commercial customized immunobead-based array was used to analyze the concentration of 23 cytokines in tear samples with a Luminex IS-100 (Luminex Corporation, Austin, TX, USA). The concentrations of interleukin (IL)-1β, IL-1 receptor antagonist (IL-1RA), IL-2, IL-4, IL-5, IL-6, chemokine C-X-C motif ligand 8 (CXCL8)/IL-8, IL-9, IL-10, IL-12p70, IL-13, IL-17A, CXCL10/interferon gamma-induced protein 10 (IP-10), chemokine C-C motif ligand 2 (CCL2)/MCP-1, CCL3/MIP1-α, CCL5/regulated on activation, normal T-cell expressed and secreted (RANTES), CCL11/eotaxin-1, chemokine C-X3-C motif ligand 1 (CX3CL1)/fractalkine, interferon gamma (IFN)- γ, matrix metalloproteinase-9 (MMP-9), tumor necrosis factor (TNF)- α, epidermal growth factor (EGF), and vascular endothelial growth factor (VEGF) were measured simultaneously with a customized 23-plex SPR assay (SPR591 HCYTO- 60K, 23X-Milliplex; Millipore). We chose these molecules based on (1) altered serum values in mercury-intoxicated patients,[2, 21, 22] (2) altered concentrations found in DE tears by our group and others,[10, 11, 13, 15, 23–30] and (3) in patients undergoing refractive surgery.[16, 31–33] The samples were analyzed following the manufacturer's low volume sample protocol that only uses 10 µl of sample/standards per assay, as previously described.[10] Data were stored and analyzed with the "Bead View Software" (Upstate-Millipore Corporation, Watford, UK). The minimum detectable concentration, based on manufacturer specifications, was 1.2 pg/ml. Molecules that were detected in less than 30% of the samples were not statistically analyzed any further. Results were compared with a similarly aged (42.4 ± 8.1 years; p = 0.1523) control group of 22 healthy males from our files who met the same criteria as the control group for corneal sensitivity.[11, 13, 15, 28, 29, 30]

2.6. Statistical analysis

Statistical analysis was performed using R software version 3.4.1 (R Foundation for Statistical Computing, Vienna, Austria). Significance level was set at 5%. Quantitative data were summarized as means and standard deviations. Ordinal values were described using medians and interquartile ranges [IQR], unless otherwise specified in the text. The normality assumption was checked by the Shapiro-Wilk test.

Data from the study group were compared to the control groups. Student's t-tests for two independent samples were used to compare differences between mean values. Levene's test was used to check homogeneity of variance, and Welch's test was used when this assumption was not valid. When normality assumptions were not supported, the nonparametric alternative, Mann-Whitney U test, was performed.

For tear cytokine analysis values out of range, the values were imputed by the regression on order statistics method. This technique performs a regression to impute low values assuming a log-normal distribution. The detection rates in the study and control groups were compared using equality of two proportions test. Cytokine expression data were transformed using the

logarithmic base 2 scale. Expression levels in the study group were compared with levels in a control group from our database. In addition, principal component and hierarchical agglomerative cluster analyses were used to explore correlation patterns among cytokine levels in the study group. To facilitate the interpretation of the clustering result, a profile analysis was conducted, testing the differences among clusters by the same methodology as the one used to compare the study and control groups.

Results

All of the 44 patients examined at the University Clinical Toxicology Unit had erethism mercurialis and peripheral nervous system alterations that were confirmed by electrophysiology. Twenty-nine of the patients had visual complaints and were consequently referred to IOBA. Preliminary observations reported that the retinal and neurophthalmic pathological findings in these patients were as follows in decreasing order of frequency: (1) decreased contrast sensitivity, (2) optic nerve involvement associated with both visual field alterations (mainly concentric constrictions) and evoked visual potential anomalies, (3) alterations in full-field and pattern electroretinography (suggesting involvement of outer and inner retinal layers), and (4) alteration in multifocal electroretinogram (indicating decreased parafoveal retinal function) (Pastor S. Lantigua Y, Coco R, et al et al. Low visual pathway alterations and neurological toxic effects after acute mercury poisoning in zinc manufacturer workers (abstract). Invest Ophthalmol Vis Sci 2019;60:259). The ocular surface pathology of these patients has not been published and is the subject of this report.

Of the 29 patients (65.9% of the original 44 patients referred to the Toxicology Department) with visual complaints, one was evaluated but excluded due to previous corneal refractive surgery in both eyes, and six others were clinically evaluated but declined to participate in this study. Therefore, a total of 22 male patients were finally included in this study, with a mean age of 42.0 ± 7.6 (range, 28–56) years. All of them were taking psychotropic drugs for their erethism mercurialis.

3.1. Clinical Tests

Results of the clinical tests are shown in Table 1. OSDI values were abnormal (> 12) in all patients except in one. The majority of patients, 14 (63.6%), had severe dry eye (DE)-related symptoms, 4 (18.18%) had moderate symptoms, and 3 (16.6%) had mild symptomatology. Conjunctival hyperemia and ocular surface integrity (corneal fluorescein and conjunctival lissamine green staining) findings were unremarkable. T-BUT was under normal values in 5 (22.7%) patients. Based on the Schirmer test, tear production was low in 3 (13.6%) patients, and based on tear lysozyme concentrations, it was low in 6 (27.3%) patients. However, tear osmolarity was abnormally elevated in 83.4% of the patients.

Table 1
Clinical Tests Results for Mercury-intoxicated Male Patients

Patient Nº/Age	Onset of Symptoms (weeks after exposure)	OSDI (range 0-100; normal < 12)	Tear Osmolarity (normal < 308 mOsms/L)	Conjunctival Redness (0–4)	T-BUT (normal ≥ 7 sec)	Corneal/ Conjunctival Staining (range 0–5)	Schirmer Test (normal > 5 mm)/ Tear Lysozyme Level (normal ≥ 1000 µm/ml)	Corneal Sensitivity Thresholds* Mechanical/ Heat/ Cold
1/ 45	10	35.00	330	0	2	0/ 1	5/ 881	165/ +2.16/ -1.12
2/ 29	12	20.80	329	0	10	0/ 0	25/ 4934	100/ +0.80/ -0.80
3/ 49	1	52.00	323	0	2	1/ 1	22/ 1369	200/ + 0.80/ -2.72
4/ 47	1	84.00	353	0	12	0/ 0	10/ 511	160/ +2.16/ -3.20
5/ 39	2	14.50	377	0	9	0/ 0	18/ 209	90/ +1.60/ -0.80
6/ 28	0	14.50	298	0	6	0/ 0	3/ 548	50/ +1.60/ -1.20
7/ 30	1	50.00	318	0	16	0/ 0	6/ 1000	85/ +4.00/ -4.00
8/ 37	1	58.30	330	0	9	1/ 1	4/ 593	190/ +1.60/ -2.40
9/ 50	2	50.00	330	1	7	0/ 0	11/ 654	172/ +2.80/ -3.52
10/ 44	2	22.90	316	0	16	0/ 0	25/1415	190/ +2.16/ -1.44
11/ 42	2	29.10	338	0	12	0/ 0	6/ 629	Not performed
12/ 52	0	27.00	400	0	14	0/ 0	15/ 1186	200/ +3.20/ -3.52
13/ 51	3	65.90	323	2	3	1/ 1	1/ 391	200/ +0.32/ -3.20
14/ 36	4	70.40	332	0	11	0/ 0	13/ 153	120/ +3.20/ -1.20
15/ 45	1	50.00	356	0	10	0/ 0	8/ 316	200/ +4.00/ -4.00
16/ 36	2	35.00	330	0	2	0/ 1	5/ 881	100/ +2.80/ -2.20
17/ 47	1	75.00	338	0	8	2/ 1	13/ 1000	142/ +2.80/ -4.00
18/ 38	4	12.00	297	0	9	0/ 0	7/ 588	200/ +3.60/ -3.20
19/ 40	3	27.00	400	0	14	0/ 0	15/ 1186	175/ +1.20/ -2.80

SD = standard deviation; IQR = interquartile range; OSDI = ocular surface disease index; T-BUT = tear break up time.

Patient Nº/Age	Onset of Symptoms (weeks after exposure)	OSDI (range 0-100; normal < 12)	Tear Osmolarity (normal < 308 mOsms/L)	Conjunctival Redness (0–4)	T-BUT (normal ≥ 7 sec)	Corneal/ Conjunctival Staining (range 0–5)	Schirmer Test (normal > 5 mm)/ Tear Lysozyme Level (normal ≥ 1000 µm/ml)	Corneal Sensitivity Thresholds* Mechanical/ Heat/ Cold
20/ 42	1	45.00	349	0	12	0/ 0	6/ 1849	200/ +2.64/ -4.00
21/ 56	2	75.00	342	0	12	1/ 1	5/ 760	130/ +1.92/ -0.56
22/ 41	1	64.50	288	2	14	1/ 1	10/ 316	35/ +4.00/ -4.00
Mean (SD)	2.54 (2.95)	44.5 (22.04)	336.23 (28.71)		9.55 (4.39)		10.59 (6.97)/ 970.90 (984.02)	147.81 (53.36)/ + 2.35 (+ 1.10)/ -2.57 (-1.24)
Median [IQR]				0 [0]		0 [0.75]/ 0 [1]		
SD = standard deviation; IQR = interquartile range; OSDI = ocular surface disease index; T-BUT = tear break up time.								

3.2. Cornea sensitivity

Mechanical threshold and thermal thresholds for heat and cold were assessed in 21 patients (42.0 ± 7.6 years old) (one patient refused to have this test performed) of the 22 patients (Tables 1, 2) and in 20 control subjects (Table 2). All of the sensitivity thresholds were significantly higher in the mercury-intoxicated patients, indicating that their corneal sensitivity was decreased

Table 2
Corneal Sensitivity Thresholds Evaluated by Non-contact Gas Esthesiometry in Mercury-intoxicated Patients (Study Group) and in a Sample of Similarly Aged Healthy Males (Control Group)

	Study Group (n = 21)			Control Group (n = 20)			
Sensitivity threshold	Mean (SD)	95% CI		Mean (SD)	95% CI		P Value
		Inferior	Superior		Inferior	Superior	
Mechanical (mL/min)	147.81 (53.36)	123.52	172.10	69.64 (43.07)	49.49	89.80	**0.0001**
Thermal hot (ºC)	+ 2.35 (+ 1.10)	+ 1.85	+ 2.85	+ 1.3 (+ 0.89)	+ 0.89	+ 1.72	**0.0018**
Thermal cold (ºC)	-2.57 (-1.24)	-3.13	-2.00	-1.83 (-1.32)	-2.45	-1.22	**0.0470**
SD = standard deviation; CI = confidence interval.							
P-values based on comparison of group means by Student's t-test.							
Bold font denotes statistical significance (P < 0.05).							

3.3. IVCM findings

IVCM was performed in 15 patients (42.8 ± 7.9 years old) out of the 22 patients. This evaluation was not possible for technical reasons in 4 patients, and 3 others did not cooperate enough to obtain good quality images. The measured parameters and mean values for each individual are shown in Table 3, and Table 4 presents comparisons with the control values.

Table 3
Corneal Morphological Data Obtained by *In Vivo* Confocal Microscopy of 21 Mercury-poisoned Patients

	Nerve Parameters					
Patient No./ Age* (years)	Density (n/mm^2)	Length (mm/mm^2)	Tortuosity (0–4)	Density of Branching (n/mm^2)	Dendritic Cell Density (n/mm^2)	Reflectivity (Gray Units)
1/ 45	9.0	10.90	3.0	6.5	3.5	99.70
2/ 29	8.0	13.77	3.0	3.0	0.5	76.29
3/ 49	4.0	19.91	3.0	0.5	0.0	92.00
4/ 47	7.0	16.05	2.0	0.0	14.0	83.97
5/ 39	4.0	11.39	1.5	0.0	3.0	98.97
6/ 28	8.0	11.99	2.0	0.5	2.0	88.22
9/ 50	4.5	9.06	2.0	0.0	12.0	79.30
10/ 44	3.5	20.51	2.0	1.0	28.5	99.50
11/ 42	6.0	11.79	1.0	0.0	0.0	93.66
12/ 52	5.0	19.45	3.0	1.0	4.5	83.42
14/ 36	2.0	26.15	3.0	0.0	5.0	101.23
17/ 47	4.0	17.78	2.0	1.0	15.5	118.75
18/ 38	13.0	16.04	3.0	5.5	23.0	104.56
19/ 40	8.5	16.81	2.0	6.5	16.5	79.02
21/ 56	9.5	16.89	2.0	4.5	8.50	97.72
Mean (SD)	6.4 (2.9)	15.90 (4.54)		2 (2.5)	9.1 (8.9)	93.09 (11.56)
Median [IQR]			2.0 [1.0]			

SD = standard deviation; IQR = interquartile range.

*The number of each patient is the same provided in Table 1.

Table 4
Comparison of Morphologic Cornea Parameters Obtained by *In Vivo* Confocal Microscopy in 15 Mercury-intoxicated Patients (Study Group) and in Control Values from Published Literature from Our Group[16,17] and Others[19]

	Study Group Mean (SD) or Median [IQR]	Control Group* Mean (SD) or Median [IQR]	P Value**
Nerve density (n/mm^2)	6.4 (2.9)	10.5 (3.3)[17]	**0.0006**
Nerve length (mm/mm^2)	15.90 (4.54)	14.50 (2.90)[19]	0.2151
Density of nerve branching (n/mm^2)	2.0 (2.5)	52.4 (26.2)[17]	**< 0.0001**
Grade of nerve tortuosity (0–4)	2.0 [1.0]	1.9 [0.8][16]	0.1201
Density of dendritic cells (n/mm^2)	9.1 (8.8)	57.5 (70.2)[17]	**0.0063**
Reflectivity (Gray units)	93.09 (11.56)	87.16 (13.10)[16]	0.1731
SD = standard deviation; IQR = interquartile range			
*Ref. 17: n = 20 (9 males); ref. 19: n = 30 (12 males); ref. 16: n = 20 (2 males). Mean ages were significantly different from study group.			
**Student's t-test (parametric) or Mann-Whitney U test (non-parametric). Bold fonts denote statistical significance (P < 0.05).			

Mercury-intoxicated patients had significantly lower nerve density and nerve branch density than did the controls (Table 4). Density of dendritic cells in corneal stroma was also decreased in the patients compared to the control subjects. Neuromas were absent in all patients. Nerve length, nerve tortuosity, and reflectivity were not significantly different from controls. Representative images of a patient and a healthy control subject from our files are shown in Fig. 1.

3.4. Analysis of tear cytokine concentrations

The detection percentage and concentration for each tear cytokine is shown in Table 5. Eotaxin, IL-10, IL-4, and MIP-1α were not statistically analyzed any further due to the very low percentage of detection (< 30%). For the remaining cytokines, there were no differences in the percentage of detection between patients and controls.

Table 5
Percentage of Detection and Concentration of Molecules Analyzed in Tears of Mercury-intoxicated Patients and Similarly Aged Healthy Male Controls

Tear Cytokine	Study Group (n = 22)			Control Group (n = 22)			P Value*
	Detection		Concentration pg/ml mean (SD)	Detection		Concentration pg/ml mean (SD)	
	n	% [95%CI]		n	% [95%CI]		
IL-1β	11	50.0 [30.72; 69.28]	47.51 (63.93)	10	45.5 [25.07; 67.33]	72.33 (220.22)	0.6247
IL-1RA	19	86.4 [64.04; 96.41]	12521.37 (34574.58)	12	57.1 [34.44; 77.41]	653.14 (1719.65)	**< 0.0001**
IL-2	14	63.6 [40.83; 81.97]	85.95 (102.30)	6	40 [17.46; 67.11]	33.19 (43.66)	0.0761
IL-4	13	59.1 [36.68; 78.52]	nc	6	28.6 [12.19; 52.31]	nc	-
IL-5	10	45.5 [25.07; 67.33]	69.65 (109.89)	9	40.9 [21.48; 63.32]	42.39 (139.25)	0.0878
IL-6	19	86.4 [64.04; 96.41]	155.08 (152.90)	22	100 [81.50; 100]	3993.07 (6380.46)	**< 0.0001**
IL-8/CXCL8	18	81.8 [58.99; 94.01]	254.03 (699.61)	11	50 [30.72; 69.28]	131.05 (267.74)	0.0856
IL-9	15	68.2 [45.12; 85.27]	74.46 (97.20)	9	60 [32.89; 82.54]	113.55 (196.47)	0.4011
IL-10	7	31.8 [14.73; 54.88]	nc	2	22.2 [3.95; 59.81]	nc	-
IL-12p70	10	45.5 [25.07; 54.88]	547.23 (550.55)	15	68.2 [45.12; 85.27]	178.84 (384.43)	**< 0.0001**
IL-13	19	86.4 [64.04; 96.41]	244.36 (259.51)	21	95.5 [75.12; 99.76]	345.72 (432.69)	0.7154
IL-17A	10	45.5 [25.07; 67.33]	111.65 (128.55)	4	80 [29.88; 98.95]	67.18 (70.24)	0.4916
IP-10/CXCL10	21	95.5 [75.12; 99.76]	18258.55 (26512.65)	21	100 [80.76; 100]	29848.1 (22155.25)	**0.0063**
MCP-1/CCL2	18	81.8 [58.99; 94.01]	1070.7 (1391.46)	10	90.9 [57.12; 99.52]	623.91 (877.95)	0.6151
MIP-1α/CCL3	4	18.2 [5.99; 41.01]	nc	0	0 [0.00; 34.45]	nc	-

SD = standard deviation; n = number of patients and controls (out of 22 in each group) for whom each molecule was detected; CI = confidence interval; nc = not calculated; IL = Interleukin; IL-1RA = IL-1 receptor antagonist; IP = induced protein; CXCL = chemokine [C-X-C motif] ligand; MCP = monocyte chemoattractant protein; CCL = Chemokine [C-C motif] ligand; MIP = Macrophage inflammatory protein; RANTES = regulated on activation, normal T cell expressed and secreted; CX3CL = chemokine [C-X3-C motif] ligand; MMP = matrix metalloproteinase; TNF = tumor necrosis factor; EGF = epidermal growth factor; VEGF = vascular endothelial growth factor; IFN = interferon.

*P value corresponding to comparison of concentrations in patient and control groups.

Significant P values (P < 0.05) are denoted in bold.

Tear Cytokine	Study Group (n = 22)			Control Group (n = 22)			P Value*
	Detection		Concentration pg/ml mean (SD)	Detection		Concentration pg/ml mean (SD)	
	n	% [95%CI]		n	% [95%CI]		
RANTES/CCL5	13	59.1 [36.68; 78.52]	743.93 (805.14)	17	81 [57.42; 93.71]	189.96 (30.68)	**0.0003**
Eotaxin/CCL11	7	31.8 [14.73;54.88]	nc	2	18.2 [3.21; 52.25]	nc	-
Fractalkine/CX3CL1	14	63.6 [40.83; 81.97	3717.06 (3935.46)	14	87.5 [60.41; 97.80]	2331.99 (2837.07)	0.4125
IFN-γ	13	59.1 [36.68; 78.52]	253.72 (369.22)	11	52.4 [30.34; 73.61]	56.63 (110.52)	*0.0521*
MMP-9	18	81.8 [58.99; 94.01]	7940.85 (32418.03)	12	92.3 [62.09; 99.60]	5172.62 (14847.46)	0.5378
TNF-α	14	63.6 [40.83; 81.97]	65.21 (89.61)	11	50.0 [30.72; 69.28]	59.36 (187.56)	0.1103
EGF	17	77.3 [54.18;91.31]	1170.76 (1340.29)	22	100 [81.50;100]	2181.59 (2494.04)	**0.0339**
VEGF	19	86.4 [64.04; 96.41]	6020.83 (4136.76)	10	66.7 [38.69; 87.01]	2068.73 (2690.54)	**< 0.0001**

SD = standard deviation; n = number of patients and controls (out of 22 in each group) for whom each molecule was detected; CI = confidence interval; nc = not calculated; IL = Interleukin; IL-1RA = IL-1 receptor antagonist; IP = induced protein; CXCL = chemokine [C-X-C motif] ligand; MCP = monocyte chemoattractant protein; CCL = Chemokine [C-C motif] ligand; MIP = Macrophage inflammatory protein; RANTES = regulated on activation, normal T cell expressed and secreted; CX3CL = chemokine [C-X3-C motif] ligand; MMP = matrix metalloproteinase; TNF = tumor necrosis factor; EGF = epidermal growth factor; VEGF = vascular endothelial growth factor; IFN = interferon.

*P value corresponding to comparison of concentrations in patient and control groups.

Significant P values (P < 0.05) are denoted in bold.

For some cytokines, i.e., IL-12p70, IL-1RA, RANTES, and VEGF, the tear concentrations were significantly higher in the patients than in the control subjects (Table 5, Fig. 2). However, for other cytokines, i.e., EGF, IL-6, and IP-10, the tear concentrations were significantly lower in the patients compared to the control subjects.

To further explore correlation patterns among tear cytokine levels in the patient samples, principal component analysis (PCA) and hierarchical agglomerative cluster analysis were performed. To accommodate much of the variance in the primary dataset, PCA was used to build a few independent principal components (PC) based on interrelated levels of the 23 cytokines. In this case, two components explained 81.6% of the sample variability, suggesting that there were two principal components (PC1 and PC2) associated with the tear cytokine levels. PC1 showed high loadings on the levels of RANTES, TNF-α, IFN-γ, IL-12p70, IL-5, IL-2, IL-1β, IL-17A, IL-6, VEGF, IL-13, fractalkine, and IL-9. However, PC2 was more correlated with IP-10, IL-8, IL-1RA, EGF, MMP-9, MCP-1, eotaxin, and IL-10 levels.

Based on PC1 and PC2, we then used hierarchical agglomerative clustering analysis to classify the patients into groups. From the resulting dendrogram (grouping tree), two optimal clusters were established. Cluster 1 consisted of 14 patients, (no. 2, 6, 7, 9–12, 15–21), and Cluster 2 consisted of 8 patients (no. 1, 3, 4, 5, 8, 13, 14, and 22). The tear cytokine concentrations in both clusters are shown in Table 6. All concentrations, except those of EGF, IL-1RA, IP-10, and MMP-9, were significantly higher in

Cluster 2. The most increased cytokine concentration in Cluster 2 was IFN-γ, which was 43.4 times higher than in Cluster 1 (Table 6).

Table 6
Cytokine Concentrations in Tears of Patients in Cluster 1 and Cluster 2

Tear Molecule	Concentration (pg/ml) Mean (Standard Deviation) / Median [Interquartile Range]		Fold Change (Log2)	Adjusted P Value
	Cluster 1 (n = 14)	Cluster 2 (n = 8)		
IL-1β	12.47 (9.89) / 9.94 [11.80]	108.82 (73) / 109.45 [73.58]	3.02	**0.0009**
IL-1RA	17918.94 (42897.86) / 1120.00 [5331.25]	3075.62 (2899.16) / 1455.00 [3310.00]	0.70	0.6152
IL-2	22.39 (18.04) / 17.99 [22.57]	197.18 (92.58) / 182.00 [43.25]	3.48	**< 0.0001**
IL-4	217.01 (191.75) / 149.35 [204.63]	1129 (774.36) / 1138.50 [1009.25]	2.57	**0.0003**
IL-5	8.95 (8.66) / 6.14 [10.52]	175.86 (125.80) / 169.00 [141.93]	4.67	**< 0.0001**
IL-6	69.05 (51.35) / 61.4 [85.19]	305.62 (156.63) / 314.50 [124.50]	2.44	**0.0001**
IL-8/CXCL8	289.27 (883.19) / 33.35 [72.04]	192.36 (113.63) / 158.00 [162.90]	2.21	**0.0144**
IL-9	19.9 (15.13) / 16.71 [23.90]	169.93 (107.48) / 156.00 [33.68]	3.34	**< 0.0001**
IL-10	61.22 (44.61) / 53.41 [67.89]	509.64 (415.36) / 535.00 [423.75]	2.62	**0.0078**
IL-12p70	195.14 (101.51) / 188.51 [172.44]	1163.38 (456.5) / 1065.00 [491.75]	2.72	**< 0.0001**
IL-13	91.64 (65.76) / 88.70 [91.02]	511.62 (256.37) / 466.50 [177.75]	2.84	**0.0001**
IL-17A	32.19 (20.14) / 29.02 [31.45]	250.71 (118.73) / 260.50 [93.50]	3.13	**< 0.0001**
IP-10/CXCL10	21081.29 (33089.71) / 10660.00 [19848.25]	13318.75 (5612.46) / 12800.00 [6342.50]	1.33	0.1529
MCP-1/CCL2	578.88 (1088.12) / 237.50 [397.44]	1931.38)1509.72) / 2065.00 [2257.75]	2.50	**0.0083**
RANTES/CCL5	224.68 (214.75) / 145.24 [118.81]	1652.62 (613.31) / 1625.00 [382.50]	3.37	**< 0.0001**
Eotaxin/CCL11	35.72 (54.9) / 19.54 [27.23]	218.59 (263.31) / 142.70 [212.31]	2.38	**0.0284**
Fractalkine/CX3CL1	1596.81 (3124.23) / 643.47 [555.99]	7427.5 (1900.32) / 7595.00 [1407.50]	3.38	**0.0001**
IFN-γ	27.2 (34.91) / 15.86 [17.22]	650.12 (352.83) / 662.50 [316.25]	5.44	**< 0.0001**

IL = Interleukin; IL-1RA = IL-1 receptor antagonist; IP = induced protein; CXCL = chemokine [C-X-C motif] ligand; MCP = monocyte chemoattractant protein = CCL = chemokine [C-C motif] ligand; MIP = macrophage inflammatory protein; RANTES = regulated on activation, normal T cell expressed and secreted; CX3CL = chemokine [C-X3-C motif] ligand; IFN = interferon; MMP = matrix metalloproteinase; TNF = tumor necrosis factor EGF = epidermal growth factor; VEGF = vascular endothelial growth factor.

*P value corresponding to comparison of tear cytokine concentration values between Cluster 1 and Cluster 2.

Significant P values (P < 0.05) are denoted in bold.

Tear Molecule	Concentration (pg/ml) Mean (Standard Deviation) / Median [Interquartile Range]		Fold Change (Log2)	Adjusted P Value
	Cluster 1 (n = 14)	Cluster 2 (n = 8)		
MMP-9	11773.76 (40665.8) / 289.00 [1937.85]	1233.25 (902.46) / 837.50 [1375.75]	1.42	0.2081
TNF-α	14.18 (11.59) / 10.67 [15.54]	154.51 (97.55) / 138.50 [48.38]	3.79	**< 0.0001**
EGF	2982.49 (8168.04) / 145.50 [2205.38]	1728.88 (1192.08) / 1895.00 [2116.25]	2.29	0.0981
VEGF	3644.16 (1891.64) / 3585.00 [2770.00]	10180 (3691.33) / 10200.00 [3345.00]	1.60	**0.0002**

IL = Interleukin; IL-1RA = IL-1 receptor antagonist; IP = induced protein; CXCL = chemokine [C-X-C motif] ligand; MCP = monocyte chemoattractant protein = CCL = chemokine [C-C motif] ligand; MIP = macrophage inflammatory protein; RANTES = regulated on activation, normal T cell expressed and secreted; CX3CL = chemokine [C-X3-C motif] ligand; IFN = interferon; MMP = matrix metalloproteinase; TNF = tumor necrosis factor EGF = epidermal growth factor; VEGF = vascular endothelial growth factor.

*P value corresponding to comparison of tear cytokine concentration values between Cluster 1 and Cluster 2.

Significant P values (P < 0.05) are denoted in bold.

The comparison of clinical parameter values between patients in each Cluster (Table 7) revealed that the maximum mercury level in urine was significantly higher in Cluster 2 (p = 0.0373). Additionally, lysozyme tear levels were significantly lower (p = 0.0189) in Cluster 2. There were also significant differences in the density of nerve branching and the density of dendritic cells, both lower in Cluster 2 (p = 0.0417 and p = 0.0291, respectively).

Table 7
Results of Clinical Tests, Esthesiometry, and Corneal Imaging in Patients Classified as Cluster 1 and Cluster 2 Based on Tear Cytokine Levels

Test	Cluster 1 (n = 14)	Cluster 2 (n = 8)	P Value
OSDI questionnaire (0-100) mean (SD)	38.09 (20.19)	55.58 (21.89)	0.0723
Tear osmolarity (mOsms/L) mean (SD)	338.64 (31.03)	332 (25.56)	0.6137
Conjunctival redness (0–4) median [IQR]	0 [0]	0 [0.5]	0.2295
T-BUT (seconds) mean (SD)	10.57 (3.98)	7.75 (4.77)	0.1517
Ocular surface integrity (0–5) median [IQR]	0 [0]	0.5 [1.0]	0.1246
Corneal staining	0 [0]	1.0 [1.0]	0.0656
Conjunctival staining			
Tear production mean (SD)	10.71 (7.14)	10.38 (7.15)	0.8372
Schirmer test (mm/5 min)	1209.79 (1143.54)	552.88 (403.12)	**0.0189**
Lysozyme tear level (µg/ml)			
Corneal sensitivity thresholds mean (SD)	149.54 (51.94)	145 (59.10)	0.8555
Mechanical (mL/min)	+ 2.58 (+ 1.01)	+ 1.98 (+ 1.20)	0.2342
Thermal hot (ºC)	-2.71 (-1.31)	-2.33 (-1.17)	0.4008
Thermal cold (ºC)			
Corneal imaging in vivo confocal microscopy	7.0 (2.9)	5.2 (2.8)	0.2786
Nerve density (n/mm^2) mean (SD)	15.41 (3.65)	16.88 (6.35)	0.5728
Nerve length (mm/mm^2) mean (SD)	2.3 (2.4)	0.1 (0.3)	**0.0417**
Nerve branching density (n/mm^2) mean (SD)	2.2 [0.6]	2.5 [0.7]	0.5034
Nerve tortuosity (0–4) median [IQR)]	11.10 (9.79)	2.88 (2.1)	**0.0291**
Dendritic cell density (n/mm^2) mean (SD)	92.05 (13.46)	95.17 (7.20)	0.6391
Reflectivity (Gray units) mean (SD)			
Maximum mercury levels* mean (SD)	398.57 (273.61)	359.75 (314.61)	0.7647
Blood (µg/L)	121.64 (121.65)	384.75 (396.88)	**0.0373**
Urine (µg/g creatinine)			
OSDI = Ocular Surface Disease Index; IQR = Interquartile range.			
*Mercury normal levels = blood < 10 µg/L and urine < 30 µg/g creatinine.			
*P value corresponding to comparison of concentration values between patient and control groups.			
Significant P values (P < 0.05) are denoted in bold.			

Discussion

In this study, we use a wide variety of techniques to describe for the first time the chronic ocular surface pathology caused by acute/subacute mercury poisoning in workers accidentally exposed to toxic doses of mercury. Briefly, we showed that most patients were highly symptomatic and had increased tear osmolarity, corneal hypoesthesia, altered corneal sub-basal nerve and

dendritic cell parameters, and altered tear levels of some inflammation-related cytokines. We concluded that the pathology encountered 1–2 years after the acute/subacute event is consistent with a neurogenic-based DE disease that was more severe in patients with higher urine levels of mercury.

The chief target organ of mercury vapor is the brain, where it causes apoptosis and ischemia of nerve fibers.[4] The eye and visual pathways are especially susceptible to neurologically-driven diseases, and the ocular effects of poisoning due to mercury exposure are not unexpected because of the extraordinarily abundant innervation of the eye. This is especially true in the cornea, the most highly innervated tissue in the whole human body. This innervation is sensitive and is delivered by the ophthalmic branch of the trigeminal or V cranial nerve.[34] Because the damage caused by mercury poisoning could target this rich innervation, we evaluated corneal sensitivity and the morphology of the sub-basal corneal nerves by non-contact esthesiometry and IVCM, respectively. Both techniques are minimally invasive, and although not regularly performed in the clinical setting, they can provide invaluable information about some ocular surface diseases. We have accumulated experience with these techniques in contact lens-related discomfort [18] and stem cell therapy for corneal pathology.[35]

Mercury poisoning, which could be responsible for the neurotoxicity and subsequent damage to the corneal nerves, could also be why the vast majority of the patients had DE-related symptoms, most of which were strongly experienced. Aside from changes in some tear cytokines (as discussed below), there were no signs of alteration in tear production and/or tear quality that can cause epithelial damage to the ocular surface as would be typical in tear-deficient and/or evaporative DE. In fact, a disparity between signs visualized with the slit lamp and symptoms is one of the most striking aspects of DE disease and has been reported in many types of DE patients.[12, 34, 36] This is especially true after corneal refractive surgery (the so-called “pain without stain”) in which there is an unavoidable lesion to the corneal nerves as part of the required laser treatment.[37] In post-refractive surgery patients, and most likely in our mercury-intoxicated patients, neurogenic inflammation due to corneal nerve damage results in the release of the inflammatory mediators.[37] This inflammation could cause the patients to have DE symptoms without manifestation of compromised tear production, and therefore not causing an obvious ocular surface integrity problem. It is not clear why corneal nerve damage and hypoesthesia caused by refractive surgery or poisons like mercury develop into neurogenic DE without epithelial involvement. This problem is especially confounding because other deleterious causes, e.g., neurotrophic keratitis, also have corneal nerve damage and reduction of corneal sensation but result in epithelial damage. We hypothesize that neurogenic DE represents either another stage or another cause of neurotrophic keratitis. Clearly, more research is needed to better understand these conditions at the molecular and genetic levels.[38]

Tear osmolarity was elevated in 19 of the 22 patients. Although tear hyperosmolarity has been implicated in the pathogenesis of DE,[12] there is no obvious explanation as to why the osmolarity was high in these patients, especially since there was no accompanying damage to the integrity of the ocular surface. Consistent with our findings, Yi et al.[39] reported a significant positive correlation between tear osmolarity and ocular symptoms, including cold sensitivity, foreign body sensation, and light sensitivity; however in our patients, T-BUT, corneal staining, eyelid hyperemia, and tear secretion volume were not significantly correlated with tear osmolarity. Similarly, Gjerdrum et al.[40] also found tear hyperosmolarity with normal tear production in patients after nerve alteration caused by corneal laser surgery.

Using Belmonte’s gas esthesiometer to measure corneal sensitivity thresholds, we found an increase in the mechanical threshold and in the heat and cold thermal thresholds in the mercury-intoxicated patients. This means that the overall corneal sensitivity was diminished. Benitez del Castillo et al.[36] found similar results for mechanical and thermal sensitivities in Sjögren syndrome-associated DE disease. Likewise, Bourcier et al.[41] reported corneal hypoesthesia with mechanical and thermal stimuli in a more mixed sample of DE patients.

The changes in corneal sensitivity are probably due to the nerve damage that we detected by IVCM. Corneal nerves not only protect the ocular surface through the mechanism of sensation, but they also release trophic factors that regulate wound healing, epithelial integrity, and cell proliferation.[19, 34, 42] Thus, nerve damage caused by mercury intoxication could be responsible for an alteration in neuronal stimulation and a delay in the transmission of nerve impulses of the affected fibers. This would explain the decrease in mechanical and thermal sensitivity that we found.

Regarding nerve morphology, corneal nerve density and nerve branch density were significantly lower in the mercury-intoxicated patients, and these changes were associated with higher levels of mercury in the urine of Cluster 2 patients. These results are in agreement with most studies in which there was a significant reduction in the sub-basal nerve density in DE patients compared with controls.[23, 43] There are, however, two studies[44, 45] that show no difference in sub-basal nerve density, but instead, the DE patients had abnormal nerve morphology. Finally, one study of patients with aqueous-deficient DE disease found increased sub-basal nerve density, suggesting the possibility of corneal nerve regeneration in this form of DE.[46] In general, regenerative activity is manifested by nerve branches from endbulbs, and in our patients, the density of branches was diminished. All of these findings support the notion that mercury intoxication adversely affects nerve function and also the capacity for nerve regeneration.

The density of dendritic cells in the corneal stroma of our mercury-intoxicated patients was decreased. Dendritic cells are in contact with the sensory nerve fibers, and play an important role in corneal homeostasis.[23, 47, 48] Elevated density of dendritic cells is a common finding in inflammatory disorders such as DE disease,[23] after refractive surgery, [49] in diabetic neuropathy,[49] and in infectious keratitis.[23] Consequently, we initially expected to find a higher density of these cells in the cornea of our patients. However, where more centralized nerve damage occurs, such as in patients with fibromyalgia syndrome where the corneal sub-basal nerve plexus is also damaged, corneal dendritic cell density is similaly decreased.[47] In animals, after trigeminal denervation, there is a depletion of dendritic cells, and corneal sensitivity is significantly reduced, delaying corneal recovery during wound healing.[48] So the decrease in the density of dendritic cells in our mercury-intoxicated patients could be due to the damage we demonstrated in corneal sub-basal nerve plexus.

Lastly, we found alterations in some tear cytokine levels in the mercury-intoxicated patients. Damage caused by mercury intoxication could be responsible for the alterations in nerve stimulation and impulse transmission. It could also cause nerve inflammation, resulting in liberation of several inflammatory cytokines. Indeed, neuro-inflammation is one of the main pathways of methyl mercury-induced central nervous system impairment.[2] Furthermore, in addition to affecting the nervous system, there is accumulating evidence that exposure to mercury alters immunomodulation, although with differences in the mechanism of action depending on the specific form of mercury (inorganic or organic), the species, and even the cell type or tissue.[2, 50] Also, other cell types apart from nerves, such as ocular epithelial and/or immune cells, could participate in the ocular surface inflammatory response to mercury exposure. These responses are related to interactions of metals, such as mercury, with electrophilic groups that are not solely restricted to the central nervous system, but are also ubiquitously present in several systems and organs.[2, 6, 7, 50]

Other studies have already shown tear molecule alterations in several ocular pathologies.[10, 11, 13, 15, 23–30] Additionally, some studies reported alteration of tear cytokine levels after corneal refractive surgery.[16, 31–33] While there are several published studies regarding serum and/or tissue cytokine/chemokine levels or gene expression in mercury-intoxicated patients, [2, 21, 22] to our knowledge, this study is the first to address tear cytokine levels in these patients.

We found that mercury-intoxicated patients had significantly increased tear levels of IL-12p70, IL-1RA, RANTES, and VEGF. Similar findings have been described in DE patients[13, 26, 51] and in tears from advanced surface ablation refractive surgery patients.[16] The increase in these molecules is in agreement with the increase in serum cytokines in mercury-exposed patients, [2, 21, 22] and it reflects an inflammatory response at the ocular surface of these patients.

On the other hand. EGF, IP-10, and IL-6 tear levels were significantly decreased in mercury-intoxicated patients. EGF tear levels usually decrease in DE patients, particularly in the more severe forms.[10, 27, 29, 30] A decrease in tear IP-10 levels has also been described by our group in patients with severe DE associated with ocular graft vs host disease[30] and by others in primary Sjögren syndrome and in Stevens-Johnson syndrome patients.[52]

The finding of decreased tear IL-6 levels is in contrast to the increased concentration in DE patients.[24, 26, 27, 29] However, a decrease in serum cytokines, including IL-6, has been reported among anti-nuclear antibody-positive subjects after mercury exposure. Nyland et al. suggested that the decrease in cytokine concentration was a specific phenotype of mercury susceptibility.[21] A recent study in mice intoxicated with mercury showed increased levels of IL-6 in serum but not in the

cerebellum.[53] IL-6 is a pleiotropic cytokine that acts as a neurotrophic factor and is crucial in the differentiation of oligodendrocytes and regeneration of peripheral nerves.[54] The decrease in IL-6 levels could be a factor contributing to the lower density of corneal nerves, branching density, and dendritic cell density observed in our patients.

In addition to the measurement of tear cytokine levels in the mercury-intoxicated patients, we performed PC and hierarchical agglomerative cluster analyses to explore correlation patterns among cytokine tear levels and the associations with the clinical findings. Based on the tear cytokine levels, we identified two patient clusters. Patients in Cluster 2 had significantly increased tear levels for 18 out of the 23 assayed cytokines, indicating a higher degree of ocular surface inflammation in this group. In agreement with this, the Cluster 2 patients also had significantly decreased tear lysozyme levels, indicating reduced tear production, compared to the patients in Cluster 1. Interestingly, in the same group, the nerve branching density and dendritic cell density were also lower than in Cluster 1. Because the maximum urine mercury levels were significantly higher in patients belonging to Cluster 2, this probably indicates a more intense mercury intoxication in dose and/or exposure time, and/or a higher susceptibility to mercury toxicity.[21]

Regarding our control groups, like the mercury-intoxicated patients, they were composed of males whose ages were not significantly different from that of the patients. IVCM was the only parameter compared with control values taken from three publications (two of them from our group), that included females and the ages were significantly different (see Table 4). While acknowledging that this is a limitation, we however feel that the comparisons are reliable because the corneal IVCM parameters that we analyzed do not change with age and are not associated with sex. [55–57]

Another potential limitation is that our patients were taking psychotropic drugs for their erethism mercurialis. Because all of the patients had a similar clinical picture and were taking similar drugs, it is unlikely that this unavoidable potential bias had any effect of the results of our evaluations.

In summary, we described a range of unreported ocular surface pathologies produced by mercury poisoning. We hypothesize that the DE-related symptoms experienced by the patients are due to mercury-related damage to the corneal innervation, corneal sensitivity, and tear cytokine disturbances. Thus, this DE could be described as neurogenic in origin, in contrast to the more classic tear-deficient and/or evaporative-DE subtypes.

Abbreviations

CCL= chemokine C-C motif ligand; **CI**= confidence interval; **CXCL=** chemokine C-X-C motif ligand; **CX3CL=** chemokine C-X3-C motif ligand; **DE=** dry eye; **EGF**= epidermal growth factor; **FC**= fold change; **IFN-g**= interferon - gamma; **IL**= Interleukin; **IL-1RA=** IL-1 receptor antagonist; **IOBA=** Institute of Applied Ophthalmobioloby; **IP-10**= interferon- gamma-induced protein-10; **IQR=** interquartile range; **IVCM=** in vivo confocal microscopy; **MCP-1**= monocyte chemoattractant protein-1; **MIP-1=** macrophage inflammatory protein-1; **MMP-9**= matrix metalloproteinase-9; **OSDI=** ocular surface disease index; **PC**= principal component; **PCA**= principal component analysis; **RANTES**= regulated on activation, normal T cell expressed and secreted; **SD=** standard deviation; **T-BUT=** tear break-up time; **TNF- a=** tumor necrosis factor alpha; **VEGF=** vascular endothelial growth factor.

Declarations

<u>Author contributions:</u>

Concept and design: MC;JCP;YL

Data acquisition: PC;YL

Data analysis /interpretation: IF;PC;YL;AES;SPI;EMS;AD; JLPC;JCP;MC

Drafting manuscript: PC;MC,AES;IF

Critical revision of manuscript: IF;PC;YL;AES;SPI;EMS;AD;JLPC;JCP;MC

Statistical analysis: IF

Supervision: PC;YL;AES;IF;SPI;EMS;AD;JLPC;JCP;MC

Final approval: PC;YL;AES;SPI;EMS;AD;IF;JLPC;JCP;MC

Meeting Presentation: “Ocular Surface Pathology in Patients Suffering from Acute Intoxication with Inorganic Mercury” Abstract No 2768 B0518. Presented in: Association for Research in Vision and Ophthalmology Annual Meeting, Vancouver, BC, Canada 2019.

Financial Support: None

Conflict of Interest: Authors have no conflict of interest with any products, techniques or drugs mentioned.

References

1. Bank, M. S. The mercury science-policy interface: History, evolution and progress of the Minamata Convention. *Sci Total Environ.* **722**, 137832 https://doi.org/10.1016/j.scitotenv.2020.137832 (2020).
2. Yang, L. *et al.* Toxicity of mercury: Molecular evidence. *Chemosphere.* **245**, 125586 https://doi.org/10.1016/j.chemosphere.2019.125586 (2020).
3. Rooney, J. P. The retention time of inorganic mercury in the brain–a systematic review of the evidence. *Toxicol Appl Pharmacol.* **274**, 425–435 https://doi.org/10.1016/j.taap.2013.12.011 (2014).
4. Bernhoft, R. A. Mercury toxicity and treatment: a review of the literature. J Environ Public Health 2012, 460508, doi:10.1155/2012/460508 (2012).
5. El-Sherbeeny, A. M., Odom, J. V. & Smith, J. E. Visual system manifestations due to systemic exposure to mercury. *Cutan Ocul Toxicol.* **25**, 173–183 https://doi.org/10.1080/15569520600860215 (2006).
6. Luschei, E. E, N. K. M., C. M. Shaw. Chronic methylmercury exposure in the monkey. *Arch Environ Health.* **32**, 6 (1977).
7. Willes, R. F. J. F. T., E. A. Nera. Neurotoxic response of infant monkeys to methylmercury. *Toxicology.* **9**, 10 (1978).
8. Kulczycka, B. Resorption of metallic mercury by the conjunctiva. *Nature.* **206**, 943 (1965).
9. Miller, K. L. *et al.* Minimal clinically important difference for the ocular surface disease index. *Arch Ophthalmol.* **128**, 94–101 https://doi.org/10.1001/archophthalmol.2009.356 (2010).
10. Pinto-Fraga, J. *et al.* Severity, therapeutic, and activity tear biomarkers in dry eye disease: An analysis from a phase III clinical trial. *Ocul Surf.* **16**, 368–376 https://doi.org/10.1016/j.jtos.2018.05.001 (2018).
11. Fernández, I. *et al.* Response profiles to a controlled adverse desiccating environment based on clinical and tear molecule changes. *Ocul Surf.* **17**, 502–515 https://doi.org/10.1016/j.jtos.2019.03.009 (2019).
12. Wolffsohn, J. S. *et al.* TFOS DEWS II Diagnostic Methodology report. *Ocul Surf.* **15**, 539–574 https://doi.org/10.1016/j.jtos.2017.05.001 (2017).
13. Enriquez-de-Salamanca, A. *et al.* Tear cytokine and chemokine analysis and clinical correlations in evaporative-type dry eye disease. *Mol Vis.* **16**, 862–873 (2010).
14. Tesón, M., Calonge, M., Fernández, I., Stern, M. E. & González-García, M. J. Characterization by Belmonte's gas esthesiometer of mechanical, chemical, and thermal corneal sensitivity thresholds in a normal population. *Invest Ophthalmol Vis Sci.* **53**, 3154–3160 https://doi.org/10.1167/iovs.11-9304 (2012).
15. la Lopez-de, A. *et al.* Corneal Sensitivity and Inflammatory Biomarkers in Contact Lens Discomfort. *Optom Vis Sci.* **93**, 892–900 https://doi.org/10.1097/opx.0000000000000784 (2016).
16. Gonzalez-Garcia, M. J. *et al.* Clinical and tear cytokine profiles after advanced surface ablation refractive surgery: A six-month follow-up. *Exp Eye Res.* **193**, 107976 https://doi.org/10.1016/j.exer.2020.107976 (2020).

17. Garcia-Gonzalez, M. *et al.* Long-term corneal subbasal nerve plexus regeneration after laser in situ keratomileusis. *J Cataract Refract Surg.* https://doi.org/10.1016/j.jcrs.2019.02.019 (2019).
18. Rosa, L. D. L. A. et al. Are Contact Lens Discomfort or Soft Contact Lens Material Properties Associated with Alterations in the Corneal Sub-Basal Nerve Plexus?. *Curr Eye Res.* **43**, 487–492 https://doi.org/10.1080/02713683.2017.1420804 (2018).
19. Oliveira-Soto, L. & Efron, N. Morphology of corneal nerves using confocal microscopy. *Cornea.* **20**, 374–384 (2001).
20. Giannaccare, G. *et al.* In vivo confocal microscopy morphometric analysis of corneal subbasal nerve plexus in dry eye disease using newly developed fully automated system. *Graefes Arch Clin Exp Ophthalmol.* https://doi.org/10.1007/s00417-018-04225-7 (2019).
21. Nyland, J. F. *et al.* Biomarkers of methylmercury exposure immunotoxicity among fish consumers in Amazonian Brazil. *Environ Health Perspect.* **119**, 1733–1738 https://doi.org/10.1289/ehp.1103741 (2011).
22. Gardner, R. M. *et al.* Mercury exposure, serum antinuclear/antinucleolar antibodies, and serum cytokine levels in mining populations in Amazonian Brazil: a cross-sectional study. *Environ Res.* **110**, 345–354 https://doi.org/10.1016/j.envres.2010.02.001 (2010).
23. Yamaguchi, T., Hamrah, P. & Shimazaki, J. Bilateral Alterations in Corneal Nerves, Dendritic Cells, and Tear Cytokine Levels in Ocular Surface Disease. *Cornea.* **35 Suppl** (1), S65–s70 https://doi.org/10.1097/ico.0000000000000989 (2016).
24. Hagan, S., Martin, E. & Enriquez-de-Salamanca, A. Tear fluid biomarkers in ocular and systemic disease: potential use for predictive, preventive and personalised medicine. *Epma j.* **7**, 15 https://doi.org/10.1186/s13167-016-0065-3 (2016).
25. Di Zazzo, A., Micera, A., De Piano, M., Cortes, M. & Bonini, S. Tears and ocular surface disorders: Usefulness of biomarkers. *J Cell Physiol.* **234**, 9982–9993 https://doi.org/10.1002/jcp.27895 (2019).
26. Lopez-Miguel, A. *et al.* Clinical and Molecular Inflammatory Response in Sjogren Syndrome-Associated Dry Eye Patients Under Desiccating Stress. *Am J Ophthalmol.* **161**, 133–141131 https://doi.org/10.1016/j.ajo.2015.09.039 (2016).
27. Lam, H. *et al.* Tear cytokine profiles in dysfunctional tear syndrome. *Am J Ophthalmol.* **147**, 198–205 https://doi.org/e191 (2009).
28. Teson, M. *et al.* Influence of a controlled environment simulating an in-flight airplane cabin on dry eye disease. *Invest Ophthalmol Vis Sci.* **54**, 2093–2099 https://doi.org/10.1167/iovs.12-11361 (2013).
29. Lopez-Miguel, A. *et al.* Dry eye exacerbation in patients exposed to desiccating stress under controlled environmental conditions. *Am J Ophthalmol.* **157**, 788–798782 https://doi.org/10.1016/j.ajo.2014.01.001 (2014).
30. Cocho, L. *et al.* Biomarkers in Ocular Chronic Graft Versus Host Disease: Tear Cytokine- and Chemokine-Based Predictive Model. *Invest Ophthalmol Vis Sci.* **57**, 746–758 https://doi.org/10.1167/iovs.15-18615 (2016).
31. Zhang, C. *et al.* Comparison of Early Changes in Ocular Surface and Inflammatory Mediators between Femtosecond Lenticule Extraction and Small-Incision Lenticule Extraction. *PLoS One.* **11**, e0149503 https://doi.org/10.1371/journal.pone.0149503 (2016).
32. Gonzalez-Perez, J., Villa-Collar, C., Gonzalez-Meijome, J. M., Porta, N. G. & Parafita, M. A. Long-term changes in corneal structure and tear inflammatory mediators after orthokeratology and LASIK. *Invest Ophthalmol Vis Sci.* **53**, 5301–5311 https://doi.org/10.1167/iovs.11-9155 (2012).
33. Chao, C. *et al.* Long-term Effects of LASIK on Corneal Innervation and Tear Neuropeptides and the Associations With Dry Eye. *J Refract Surg.* **32**, 518–524 https://doi.org/10.3928/1081597x-20160603-01 (2016).
34. Cruzat, A., Qazi, Y. & Hamrah, P. In Vivo Confocal Microscopy of Corneal Nerves in Health and Disease. *Ocul Surf.* **15**, 15–47 https://doi.org/10.1016/j.jtos.2016.09.004 (2017).
35. Calonge, M. *et al.* A proof-of-concept clinical trial using mesenchymal stem cells for the treatment of corneal epithelial stem cell deficiency. *Transl Res.* **206**, 18–40 https://doi.org/10.1016/j.trsl.2018.11.003 (2019).
36. Benitez-Del-Castillo, J. M. *et al.* Relation between corneal innervation with confocal microscopy and corneal sensitivity with noncontact esthesiometry in patients with dry eye. *Invest Ophthalmol Vis Sci.* **48**, 173–181 https://doi.org/10.1167/iovs.06-0127 (2007).

37. Nettune, G. R. & Pflugfelder, S. C. Post-LASIK tear dysfunction and dysesthesia. *Ocul Surf.* **8**, 135–145 https://doi.org/10.1016/s1542-0124(12)70224-0 (2010).
38. Dua, H. S. *et al.* Neurotrophic keratopathy. *Prog Retin Eye Res.* **66**, 107–131 https://doi.org/10.1016/j.preteyeres.2018.04.003 (2018).
39. Yi, H. C., Lee, Y. P. & Shin, Y. J. Influence of Nasal Tear Osmolarity on Ocular Symptoms Related to Dry Eye Disease. *Am J Ophthalmol.* **189**, 71–76 https://doi.org/10.1016/j.ajo.2018.02.008 (2018).
40. Gjerdrum, B., Gundersen, K. G., Lundmark, P. O., Potvin, R. & Aakre, B. M. Prevalence of Signs and Symptoms of Dry Eye Disease 5 to 15 After Refractive Surgery. *Clin Ophthalmol.* **14**, 269–279 https://doi.org/10.2147/opth.s236749 (2020).
41. Bourcier, T. *et al.* Decreased corneal sensitivity in patients with dry eye. *Invest Ophthalmol Vis Sci.* **46**, 2341–2345 https://doi.org/10.1167/iovs.04-1426 (2005).
42. Labetoulle, M. *et al.* Role of corneal nerves in ocular surface homeostasis and disease. *Acta Ophthalmol.* **97**, 137–145 https://doi.org/10.1111/aos.13844 (2019).
43. Labbe, A. *et al.* The relationship between subbasal nerve morphology and corneal sensation in ocular surface disease. *Invest Ophthalmol Vis Sci.* **53**, 4926–4931 https://doi.org/10.1167/iovs.11-8708 (2012).
44. Tuominen, I. S. *et al.* Corneal innervation and morphology in primary Sjogren's syndrome. *Invest Ophthalmol Vis Sci.* **44**, 2545–2549 https://doi.org/10.1167/iovs.02-1260 (2003).
45. Tuisku, I. S., Konttinen, Y. T., Konttinen, L. M. & Tervo, T. M. Alterations in corneal sensitivity and nerve morphology in patients with primary Sjogren's syndrome. *Exp Eye Res.* **86**, 879–885 https://doi.org/10.1016/j.exer.2008.03.002 (2008).
46. Zhang, M. *et al.* Altered corneal nerves in aqueous tear deficiency viewed by in vivo confocal microscopy. *Cornea.* **24**, 818–824 https://doi.org/10.1097/01.ico.0000154402.01710.95 (2005).
47. Klitsch, A. *et al.* Reduced association between dendritic cells and corneal sub-basal nerve fibers in patients with fibromyalgia syndrome. *J Peripher Nerv Syst.* **25**, 9–18 https://doi.org/10.1111/jns.12360 (2020).
48. Gao, N., Lee, P. & Yu, F. S. Intraepithelial dendritic cells and sensory nerves are structurally associated and functional interdependent in the cornea. *Sci Rep.* **6**, 36414 https://doi.org/10.1038/srep36414 (2016).
49. Patel, D. V. & McGhee, C. N. In vivo confocal microscopy of human corneal nerves in health, in ocular and systemic disease, and following corneal surgery: a review. *Br J Ophthalmol.* **93**, 853–860 https://doi.org/10.1136/bjo.2008.150615 (2009).
50. Gardner, R. M., Nyland, J. F. & Silbergeld, E. K. Differential immunotoxic effects of inorganic and organic mercury species in vitro. *Toxicol Lett.* **198**, 182–190 https://doi.org/10.1016/j.toxlet.2010.06.015 (2010).
51. Na, K. S., Mok, J. W., Kim, J. Y., Rho, C. R. & Joo, C. K. Correlations between tear cytokines, chemokines, and soluble receptors and clinical severity of dry eye disease. *Invest Ophthalmol Vis Sci.* **53**, 5443–5450 https://doi.org/10.1167/iovs.11-9417 (2012).
52. Gurumurthy, S., Iyer, G., Srinivasan, B., Agarwal, S. & Angayarkanni, N. Ocular surface cytokine profile in chronic Stevens-Johnson syndrome and its response to mucous membrane grafting for lid margin keratinisation. *Br J Ophthalmol.* **102**, 169–176 https://doi.org/10.1136/bjophthalmol-2017-310373 (2018).
53. Muniroh, M. *et al.* Activation of MIP-2 and MCP-5 Expression in Methylmercury-Exposed Mice and Their Suppression by N-Acetyl-L-Cysteine. *Neurotox Res.* **37**, 827–834 https://doi.org/10.1007/s12640-020-00174-4 (2020).
54. Rothaug, M., Becker-Pauly, C. & Rose-John, S. The role of interleukin-6 signaling in nervous tissue. *Biochim Biophys Acta.* **1863**, 1218–1227 https://doi.org/10.1016/j.bbamcr.2016.03.018 (2016).
55. Erie, J. C., McLaren, J. W., Hodge, D. O. & Bourne, W. M. The effect of age on the corneal subbasal nerve plexus. *Cornea.* **24**, 705–709 (2005).
56. Gambato, C. *et al.* Aging and corneal layers: an in vivo corneal confocal microscopy study. *Graefes Arch Clin Exp Ophthalmol.* **253**, 267–275 https://doi.org/10.1007/s00417-014-2812-2 (2015).
57. Parissi, M. *et al.* Standardized baseline human corneal subbasal nerve density for clinical investigations with laser-scanning in vivo confocal microscopy. *Invest Ophthalmol Vis Sci.* **54**, 7091–7102 https://doi.org/10.1167/iovs.13-12999 (2013).

Figures

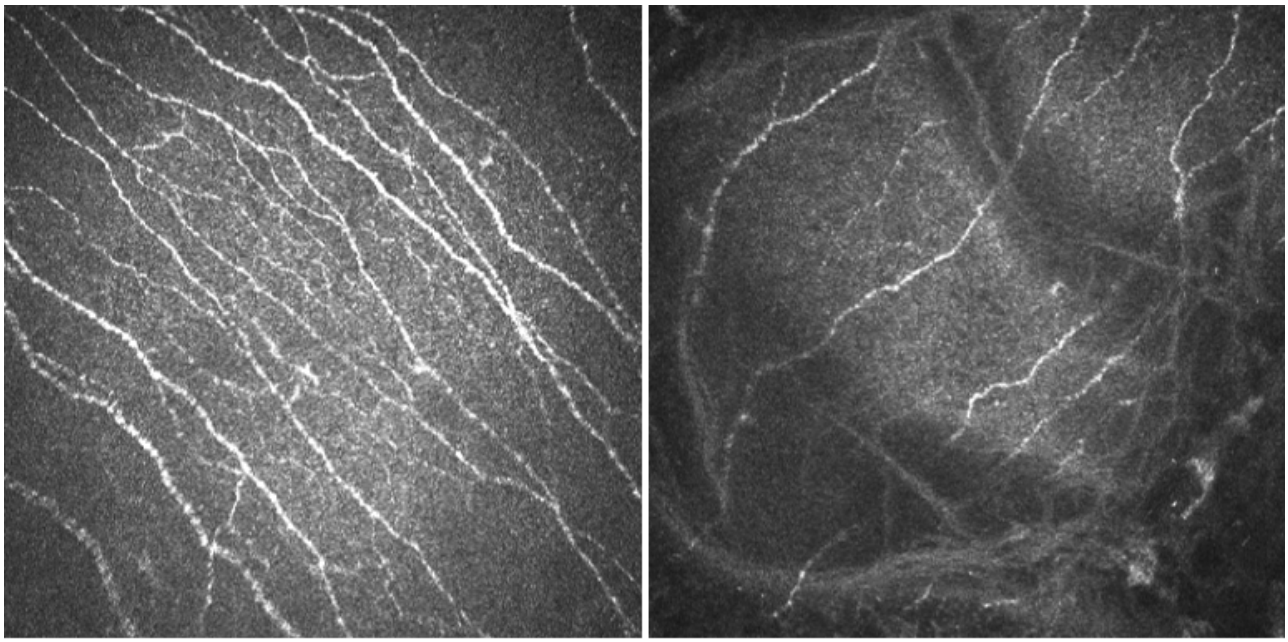

Figure 1

In vivo confocal microscopy images of the central cornea in a healthy control and in a mercury-intoxicated patient. For both corneas, the images were taken at a depth of 50-80 μm. (Left) In the healthy control subject, the following measurements were made: Nerve density, 15/mm2; Tortuosity, 2; Mean nerve length, 27.94 mm/mm2; Nerve branch density, 7/mm2; Dendritic cell density, 4/mm2; and Reflectivity, 109.1 Gray units. (Right) In the mercury-intoxicated subject, the following measurements were made: Nerve density, 8/mm2; Tortuosity, 3; Mean nerve length, 13.77 mm/mm2; nerve branch density, 3/mm2; dendritic cell density, 0.5/mm2; and Reflectivity, 76.29 Gray units.

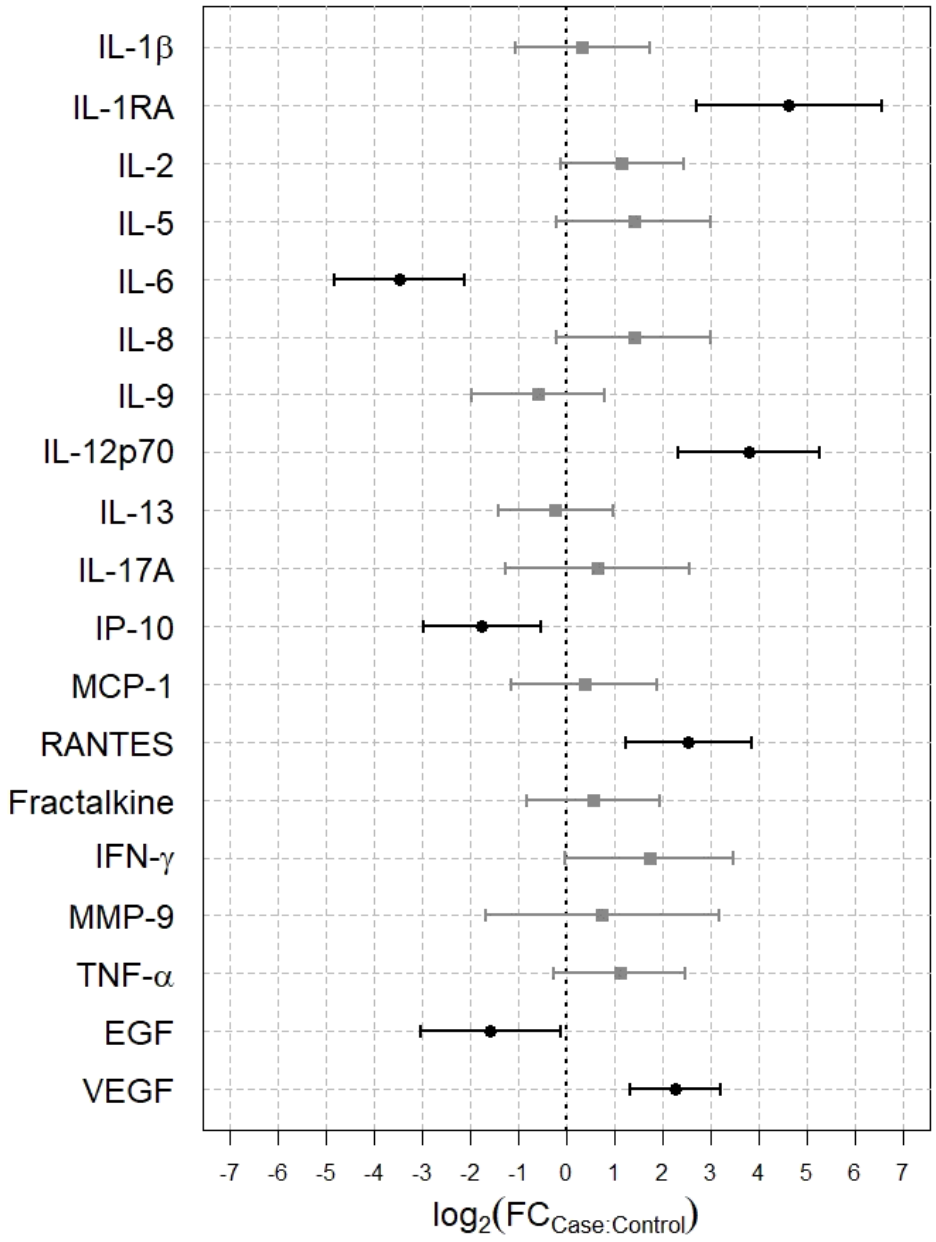

Figure 2

Fold change of tear cytokine levels in mercury-poisoned patients versus healthy controls. Tear cytokines are shown on the Y-axis. The fold change (FC) with the 95% confidence interval (CI, horizontal lines) for each cytokine is shown on the X-axis. The case:control FC was defined as the relative expression of the cytokine concentration in the patient group divided by the control group. Data on the X-axis are presented in a base 2 logarithmic (log2) scale. The vertical dashed line represents no change. The FCs were significant if the 95%CI did not cross the vertical dashed line. The farther the distance to the vertical dashed line, the greater the statistical significance. Positive values mean over-expression and negative values mean under-expression.

Supplementary Files

This is a list of supplementary files associated with this preprint. Click to download.

- AditionalInformation.docx